CHEMBIOCHEM

DOI: 10.1002/cbic.200800833

Biomolecular Oxidative Damage Activated by Enzymatic Logic Systems: Biologically Inspired Approach

Jian Zhou,[a] Galina Melman,[a] Marcos Pita,[a] Maryna Ornatska,[a] Xuemei Wang,[b] Artem Melman,*[a] and Evgeny Katz*[a]

Systems that perform oxidative damage to biomolecules through catalytic cascades in the presence of iron-redox labile species were activated by enzymatic logic gates that process chemical input signals according to built-in logic operations. **AND**/**OR** enzymatic logic gates were composed of glucose oxidase (GOx) and GOx/esterase, respectively. The **AND**/**OR** logic functions of the enzyme gates were activated by application of glucose–oxygen and glucose–ethyl acetate input signals, respectively. The enzymatic logic gates, upon activation by specific patterns of the chemical input signals, produced acidic solutions and triggered release of redox labile iron species from a complex that is unstable under acidic conditions. This resulted in the activation of a catalytic cascade, which produced reactive oxygen species (ROS) and subsequently yielded oxidative damage in biomolecules. Functional integration of the enzyme-based logic systems with the catalytic redox cascade that performs damage in biomolecules on demand is a first step towards "smart" systems capable of programmed detection, identification, and neutralization of potential biohazards.

Introduction

The recently developed concept of enzymatic logic gates,[1–3] which are a part of general research areas of biochemical[4–6] and chemical computing,[7–9] is aimed at controlling various processes and systems through logically processed biochemical signals. Information processing by biochemical reactions that perform Boolean logic operations has resulted in the design of various enzymatic logic gates (for example, **AND**, **OR**, **XOR**, **INHIB**, **NOR**).[1–3] Their networks are composed of several concatenated logic gates that perform a sequence of logic operations and can process many biochemical input signals applied in different combinations.[10,11] The logic operations performed by the enzymatic systems have already been used to trigger changes in different bioelectronic systems[12,13] and nanostructured signal-responsive materials.[14–16] Enzymatic systems that process biochemical input signals and perform Boolean logic operations could be coupled with external signal-responsive materials through an exchange of electrons or protons.[16] In our recently designed enzymatic logic gates we used pH changes generated in situ by the enzymatic systems to switch different pH-responding materials and bioelectronic systems between inactive and active states.[12–15] In the present paper we use enzymatic logic systems that transform chemical input signals into pH changes, which trigger the catalytic generation of ROS and thus result in oxidative damage in biomolecules.

Formation of ROS such as oxygen anions, peroxides, and free radicals is an unavoidable part of aerobic metabolism, and ROS play a dual role, as they are both deleterious and beneficial. Overproduction of ROS results in depletion of cellular glutathione and subsequent oxidative damage to cellular organelles. Oxidative damage by ROS has been found to be an important primary or secondary process in aging[17,18] as well as in development of a number of pathologies.[19–23] The toxicity of ROS is potentiated by labile iron cations which catalyze the formation of hydroxyl radicals capable of directly attacking cellular components; this results in DNA damage,[24–27] lipid peroxidation,[28] and protein oxidation.[29]

At the same time ROS are essential for living organisms as they participate in vitally important processes of catabolism and neutralization of pathogens. Destruction of phagocyted pathogens by ROS and proteases is the final step of phagocytosis after recognition of the pathogen and engulfing it into lysosomes, or "suicide bags." ROS are generated in lysosomes by NADPH oxidase, which is expressed in all macrophages.[30–32] Subsequent mobilization of labile iron cations by destabilization of iron-sulfur-containing enzymes[33] results in production hydroxyl radicals which inactivate phagocyted pathogens. The indiscriminate destruction of pathogens through oxidative damage is less prone to bacterial or viral resistance and may be the essential advantage over more specific immune mechanisms.[34] Integration of enzymatic logic systems with destruc-

[a] *J. Zhou, Dr. G. Melman, Dr. M. Pita, Dr. M. Ornatska, Prof. A. Melman, Prof. E. Katz*
Department of Chemistry and Biomolecular Science and NanoBio Laboratory (NABLAB), Clarkson University
Potsdam, NY 13699-5810 (USA)
Fax: (+1) 315-2686610
E-mail: ekatz@clarkson.edu
amelman@clarkson.edu

[b] *Prof. X. Wang*
State Key Laboratory of Bioelectronics, Southeast University
Nanjing 210096 (China)

Supporting information for this article is available on the WWW under http://dx.doi.org/10.1002/cbic.200800833.

tive ROS-based mechanisms might pave the road towards "smart" logic protective systems.

In this article we report on the systematic modeling of chemical defence through ROS generation triggered by enzymatic logic gates; these logic gates can process multiple biochemical signals mediated by pH change. Change of pH is capable of actuating important transformations such as conversion of iron cations from redox-inactive complexes into a redox-labile state. The redox-labile iron is capable of generating highly reactive hydroxyl radicals through the Fenton reaction with hydrogen peroxide or organic peroxides. The resulting Fe^{III} cations are reduced by superoxide anions; this produces hydrogen peroxide and regenerates Fe^{II} species, and thus results in a catalytic cycle responsible for biomolecular oxidative damage.[35,36] Usually this process is modelled by ascorbate–iron–air system[37] in which Fe^{II} species are oxidized by oxygen to yield Fe^{III} and H_2O_2. The Fe^{III} species are regenerated by ascorbate followed by Fenton reaction, thus producing hydroxyl radicals in the catalytic cycle. The catalytic cycle can be inhibited by chelation of iron cations,[38,39] as for example in iron-sulfur proteins, although many known iron ligands such as phenanthroline, nitrilotriacetic acid (NTA), or EDTA are not capable of preventing the formation of ROS and were reported to substantially potentiate oxidative damage.[40,41] The release of iron cations from a complex could be employed to activate its participation in the catalytic production of ROS. Deactivation of iron species can be achieved with deferoxamine[42] and other hexadentate hydroxamate ligands.[43,44] However, the resulting iron complexes are stable in a wide pH range and cannot be used to release active iron species on demand by varying pH mildly by the enzymatic logic systems. Recently reported new 2,6-*bis*-[hydroxy(methyl)amino]-1,3,5-triazine (BHT) iron ligands[45] have been shown to possess a special set of properties. Fe^{III} complexes of BHT ligands have both very low Fe^{II}/Fe^{III} redox potential at neutral pH and strong pH dependency of the dissociation constant.[46] In this article we report on the functional coupling of pH-labile 2:1 BHT–Fe^{III} complexes with enzymatic logic gates in situ. Catalytic production of ROS is triggered and oxidative damage is produced for biomolecules by altering pH values and releasing the active Fe^{III} cations. The present "smart" system is capable of generating oxidative damage on demand after activation by specific combinations of biochemical signals logically processed by enzymes.

Results and Discussion

The enzymatic logic gates were reported to shift pH values from neutral to acidic in the pH range of 4–7.[12–15] To adjust the pH-dependent decomposition of the Fe^{III}–$(BHT)_2$ complex to this pH range we applied NTA as a competing iron ligand to yield the redox labile Fe^{III}–(NTA) complex, Scheme 1. The pH-dependent stability of the 2:1 2,6-*bis*-[hydroxy(methyl)amino]-4-(*N*-methyl,*N*-ethoxycarbonyl)amino-1,3,5-triazine iron complex, Fe^{III}–$(BHT)_2$,[46] was studied by titration of the complex solution to different pH values in the presence of NTA. The experiment was started at pH 7.2, at which the complex is stable and shows a characteristic broad metal-to-ligand charge-transfer (MLCT) absorbance band with λ_{max} at 535 nm. Acidification of the complex solution to pH <7 resulted in the decomposition of the complex; this was monitored by disappearance of its absorbance at 535 nm, Figure 1. When the pH value reached 5.1, the complex was fully decomposed and yielded the redox-labile Fe^{III}–(NTA) complex. These results ensured that the pH-controlled release of the redox-labile iron species from the complex can be induced by pH changes produced by enzymatic reactions. The catalytic cascade resulting in the formation of ROS in the presence of the released Fe^{III}–(NTA) is outlined in Scheme 1.

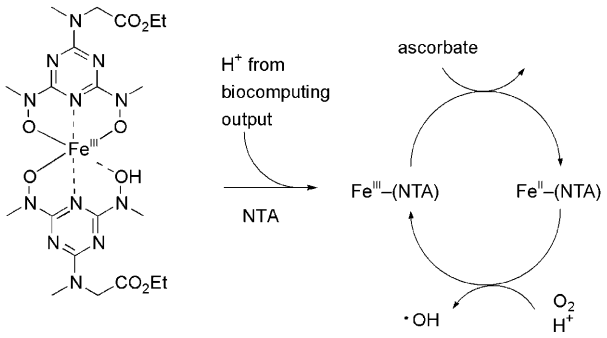

Scheme 1. Structure and decomposition of Fe^{III}–$(BHT)_2$ complex and catalytic generation of ROS by the iron–air–ascorbate system.

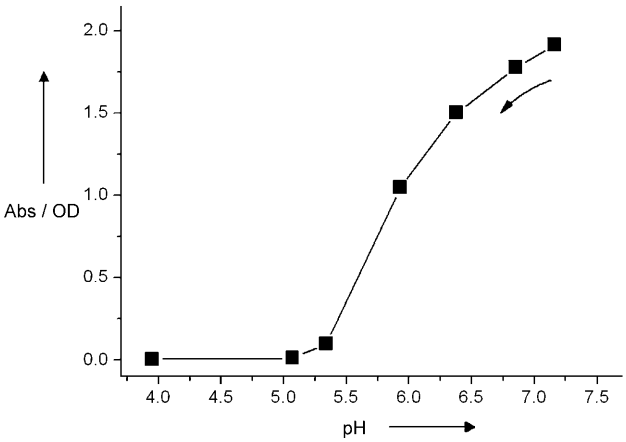

Figure 1. Decomposition of Fe^{III}–$(BHT)_2$ as monitored by its pH titration carried through the disappearance of its characteristic band with maximum at $\lambda = 535$ nm. The pH value of the solution was adjusted by addition of 0.01 M HCl.

In the present study we used glucose oxidase (GOx, 10 units mL^{-1}) to mimic Boolean **AND** logic operation upon additions of glucose, 20 mM, and oxygen (in equilibrium with air) as the input signals, Scheme 2A. The input signals were considered to be "**0**" in the absence of the respective chemicals (when necessary, the solution was deoxygenated with argon), while the input signals were "**1**" in the presence of the added chemicals at the selected concentrations. Glucose oxidation by oxygen was biocatalyzed by GOx and the formation of gluconic acid resulted in the lowering pH value of the solution. The

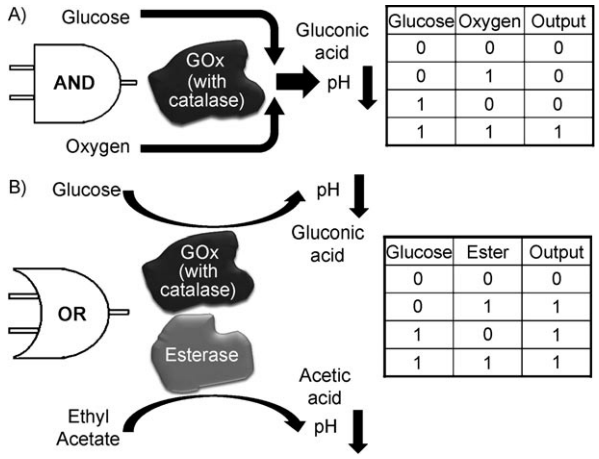

Glucose	Oxygen	Output
0	0	0
0	1	0
1	0	0
1	1	1

Glucose	Ester	Output
0	0	0
0	1	1
1	0	1
1	1	1

Scheme 2. Schematic representations of the enzymatic logic gates. A) **AND** gate formed with GOx where the combination of two inputs, glucose and oxygen, produces gluconic acid. Truth table for the **AND** logic operation is shown. B) **OR** gate formed with GOx and Est where the appearance of any input, glucose or ethyl acetate, produces gluconic acid or acetic acid, respectively. Truth table for the **OR** logic operation is shown. Cat was added to the both gates to decompose H_2O_2.

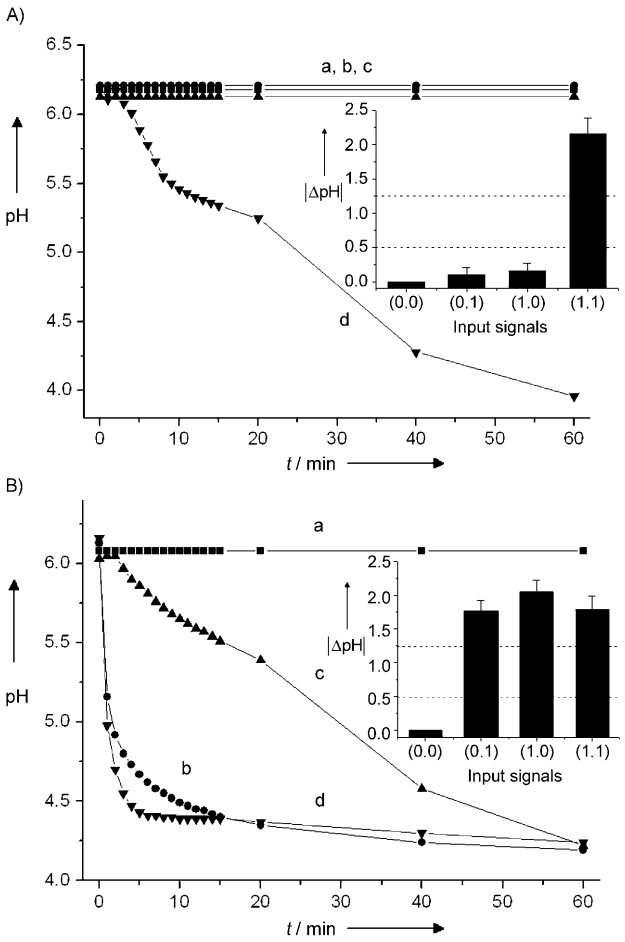

Figure 2. Generated in situ pH changes upon application of different combinations of chemical input signals: A) **AND** gate activated by glucose and O_2: a) **0,0**; b) **0,1**; c) **1,0**; d) **1,1**. B) **OR** gate activated by glucose and ethyl acetate: a) **0,0**; b) **0,1**; c) **1,0**; d) **1,1**. Insets represent the absolute value of the pH changes reaching the saturated values. The dashed lines show the threshold values for the logic **0** and **1** outputs. The solutions compositions and the input signal concentrations are specified in the experimental section.

operating concentrations of the chemical inputs (glucose and oxygen) were selected to produce substantial pH changes in a non-buffered solution (0.01 M Na_2SO_4) upon the biochemical reaction. The reaction proceeded only in the presence of both reacting components (input signals **1**,**1**) and reached a final pH of 4, while in the absence of any of the reactants or both of them (input signals **0**,**1**, **1**,**0**, **0**,**0**, respectively) the reaction was not activated and the initial pH value was unchanged at 6.1–6.2 (Figure 2A). The system responses corresponded to the Boolean **AND** logic operation (Scheme 2A truth table), in which the pH change was considered as the output signal, Figure 2A, inset. It should be noted that apart from gluconic acid, GOx produces hydrogen peroxide, which in the presence of the redox labile iron species generates hydroxyl radicals in addition to those radicals formed by the iron-air catalytic system outlined in Scheme 1. To avoid the second catalytic path and to be sure about the mechanism of the catalytic cascade and results elucidation, hydrogen peroxide produced in the reaction was rapidly decomposed by catalase present in a large excess (Cat, 250 units mL^{-1}).

Another system composed of two enzymes operating together, esterase (Est) and GOx, was activated by the additions of ethylacetate (20 mM) and glucose (20 mM) (while O_2 was always present in the system) and mimicked Boolean **OR** logic operation, Scheme 2B. Two parallel reactions, oxidation of glucose biocatalyzed by GOx and hydrolysis of ethylacetate by Est, resulted in the formation of gluconic acid or acetic acid, respectively; this resulted in a decrease in pH to acidic values of 4.2–4.3. Acid formation was achieved in both reactions, thus yielding the acidic medium in the presence of any of two substrates or both of them together (input signals **0**,**1**, **1**,**0**, **1**,**1**). Only in the absence of both inputs was the initial pH value preserved at 6.1 (input signals **0**,**0**), Figure 2B. Thus, the system responses corresponded to the Boolean **OR** logic operation (Scheme 2B truth table) when the pH change was considered as the output signal, Figure 2B, inset. Hydrogen peroxide produced upon biocatalytic oxidation of glucose was rapidly decomposed by the added catalase (Cat, 250 units mL^{-1}) for the same reason discussed above.

It should be noted that only two concentrations of the chemical input signals (corresponding to the digital values of **0** and **1**) were applied, while their intermediate concentrations were considered digitally undefined in the same way as an electrical signal in electronic logic gates is undefined while being between two threshold limits. Variation of the signal concentrations between zero and operational values (between "**0**" and "**1**" input signals) would result in a surface-response function of the logic gates, which can be used for the optimization of the gate performance;[47] this was outside the scope of the present study.

The pH changes generated in situ by the enzymatic logic systems mimicking the **AND**/**OR** logic gates were used to trigger catalytic redox reactions, Scheme 1, resulting in the biomo-

lecular oxidative damage. The process started from the pH-induced decomposition of Fe^{III}–$(BHT)_2$ complex monitored by the absorbance decrease at $\lambda_{max}=535$ nm, Figure 3. The enzymatic logic gate **AND** (composed of GOx, 10 units mL^{-1}) does not change the initial, almost neutral pH value upon application of the input signals **0**,**0**, **0**,**1** and **1**,**0**, thus preserving the Fe^{III}–$(BHT)_2$ complex in its original state with an optical density of 0.145 (Figure 3A, curves a–c). Simultaneous addition of glucose and oxygen (input signals **1**,**1**) to the system results in the formation of gluconic acid, thus lowering the pH value (reaching pH about 4.3) and resulting in the decomposition of Fe^{III}–$(BHT)_2$. This is reflected by the decrease of its absorbance at $\lambda_{max}=535$ nm to 0.023 optical density (Figure 3A, curve d). The features of the system responding to the chemical input signals resemble the logic operation **AND**, Figure 3A, inset.

The enzymatic logic gate **OR** (composed of GOx, 10 units mL^{-1} and Est, 10 units mL^{-1}) did not change the initial pH value in the absence of the both chemical signals: glucose and ethylacetate (input signals **0**,**0**), thus preserving the initial optical density of Fe^{III}–$(BHT)_2$ at 0.13 (Figure 3B, curve a). The presence of any of the chemical inputs or both of them (input signals **0**,**1**, **1**,**0**, **1**,**1**) resulted in the formation of acids. Lowering the pH from its initial almost neutral value and reaching the acidic pH of about 4.3 resulted in the decomposition of Fe^{III}–$(BHT)_2$, as observed by the optical density reduction to 0.03 at $\lambda_{max}=535$ nm (Figure 3B, curves b–d). The features of the system responding to the chemical input signals mimic the logic operation **OR**, Figure 3B, inset.

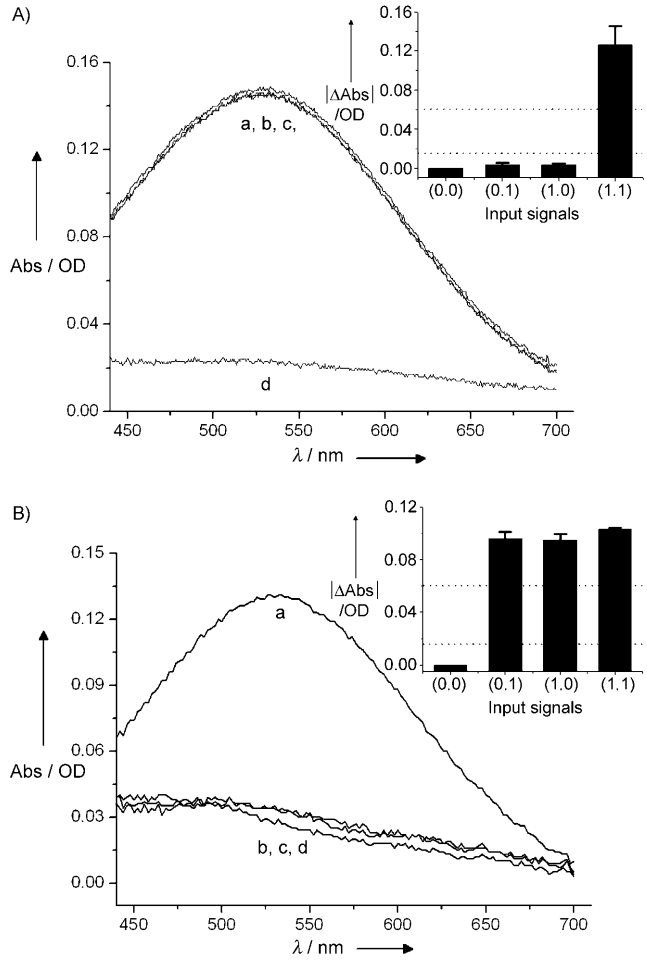

Figure 3. Absorption spectra of the Fe^{III}–$(BHT)_2$ (0.6 mM), obtained after application of different combinations of chemical input signals triggering the enzymatic logic gates: A) **AND** gate activated by glucose and O_2: a) **0**,**0**; b) **0**,**1**; c) **1**,**0**; d) **1**,**1**. B) **OR** gate activated by glucose and ethyl acetate: a) **0**,**0**; b) **0**,**1**; c) **1**,**0**; d) **1**,**1**. The insets show the absolute values of the optical absorbance changes at $\lambda=535$ nm induced by different combinations of the input signals. The dashed lines show the threshold values for the logic **0** and **1** outputs. The solutions compositions and the input signal concentrations are specified in the experimental section.

The Fe^{III} cations released from Fe^{III}–$(BHT)_2$ upon pH changes produced in situ by the enzymatic logic systems were re-chelated by NTA; this yielded the redox mobile Fe^{III}–(NTA) complex, which participated in the catalytic generation of ROS (Scheme 1). The produced Fe^{III}–(NTA) complex was immediately reduced by ascorbate and capable of participating in the Fenton reaction, which yielded OH radicals that were detected by in situ hydroxylation of benzoate.[48,49] The reaction produces a mixture of 4- and 3-hydroxybenzoates. Due to the strong fluorescence of both reaction products, the hydroxylation is a very sensitive method for the quantitative analysis of OH radicals. Figure 4A (curves a–c) shows no formation of the fluorescent products when the input signals **0**,**0**, **0**,**1**, and **1**,**0** were applied to the enzymatic logic **AND** gate. Simultaneous addition of glucose and oxygen (input signals **1**,**1**) resulted in the formation of gluconic acid and acidification of the solution, thus yielding Fe^{III}–(NTA) and inducing catalytic formation of OH radicals. This was reflected by the formation of the fluorescent products in the hydroxylation of benzoate that emits at $\lambda_{max}=$ 435 nm (Figure 4A, curve d). The system response to the chemical signals mimics the logic operation **AND** (Figure 4A, inset). When the enzymatic logic **OR** gate was used, the system did not show the fluorescent products upon application of a **0**,**0** combination of the input signals (Figure 4B, curve a), while the input signals **0**,**1**, **1**,**0**, and **1**,**1** resulted in the production of the strongly fluorescent products (Figure 4B, curves b–d). The system response to the chemical input signals mimics the logic operation **OR** (Figure 4B, inset). The fluorescent products were generated through a sequence of events starting from the enzyme induced acidification of the solution, followed by the decomposition of Fe^{III}–$(BHT)_2$, release of Fe^{III}–(NTA) and its participating in the catalytic formation of OH radicals. The formation of the fluorescent product reflects the production of OH radicals proceeded in parallel with the pH changes induced in situ by the enzyme reactions (Figures S1–S3 in the Supporting Information). These findings support the formation of the ROS triggered by the logic operations performed by the enzymatic systems processing chemical input signals.

In the next step of our research we further demonstrated that biomolecular oxidative damage can be controlled by the enzymatic logic gates. A number of methods have been reported for detection of hydroxyl radicals in cellular[50] and cell-free systems.[51,52] In cell-free systems, hydroxylation of deoxyribose[53–55] can be considered to be the most relevant method, as it models the process of DNA strain breaks. Degradation of

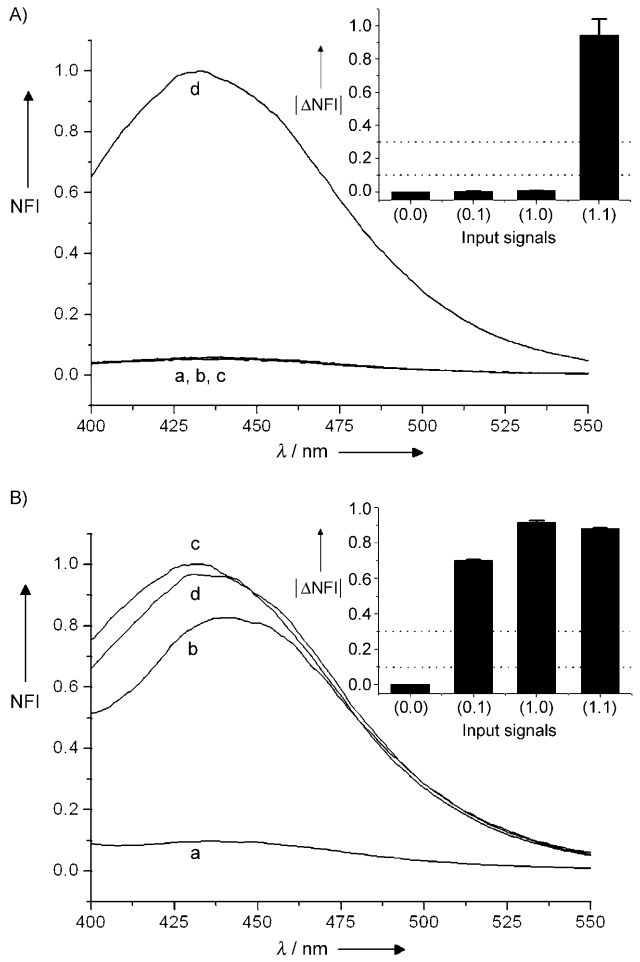

Figure 4. Normalized fluorescent intensity (NFI) generated upon reacting benzoic acid (1 mM) with Fe^{III}–$(BHT)_2$ and the enzymatic logic gates activated by different combinations of input signals: A) **AND** gate activated by glucose and O_2: a) **0,0**; b) **0,1**; c) **1,0**; d) **1,1**. B) **OR** gate activated by glucose and ethyl acetate: a) **0,0**; b) **0,1**; c) **1,0**; d) **1,1**. The insets show the changes in the NFI induced by different combinations of the input signals. The dashed lines show the threshold values for the logic **0** and **1** outputs. The solutions compositions and the input signal concentrations are specified in the experimental section.

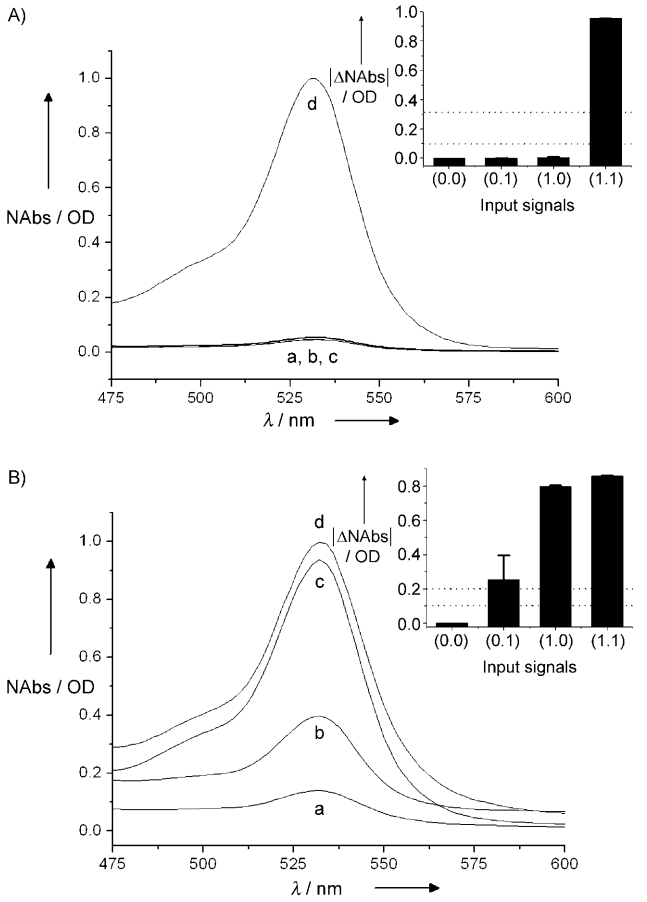

Figure 5. Normalized absorbance (NAbs) generated upon reacting deoxyribose (10 mM) with the Fe^{III}–$(BHT)_2$ and the enzymatic logic gates activated by different combinations of input signals: A) **AND** gate activated by glucose and O_2: a) **0,0**; b) **0,1**; c) **1,0**; d) **1,1**. B) **OR** gate activated by glucose and ethyl acetate: a) **0,0**; b) **0,1**; c) **1,0**; d) **1,1**. The insets show the changes in the NABs induced by different combinations of the input signals. The dashed lines show the threshold values for the logic **0** and **1** variants. The solutions compositions and the input signal concentrations are specified in the Experimental Section.

deoxyribose caused by in situ-generated ROS[53–55] was determined by the standard assay using condensation of the resultant malonic dialdehyde with thiobarbituric acid (Figure 5 A), which produced UV-Vis absorption with $\lambda_{max} = 532$ nm.[56] The enzymatic logic **AND** gate generated the ROS only upon application of the **1,1** combination of the chemical input signals, thus resulting in the oxidative damage on deoxyribose (Figure 5 A, curve d). All other combinations of the chemical input signals (**0,0**, **0,1**, **1,0**) did not yield ROS and did not produce the damaged biomolecules (Figure 5 A, curves a–c). Figure 5 A, inset, shows the system response pattern characteristic of the **AND** Boolean logic gate. The enzymatic logic **OR** gate resulted in the ROS and damaged biomolecules at **0,1**, **1,0**, and **1,1** combinations of the input signals (Figure 5 B, curves b–d), while only **0,0** input signals preserved the undamaged biomolecules (Figure 5 B, curve a). Figure 5 B, inset, shows the system response pattern characteristic of the **OR** Boolean logic gate.

Conclusions

This study illustrates the possibility to trigger biochemical processes, specifically oxidative damage, by processing chemical input signals using enzymatic systems with built in Boolean logic. The **AND**/**OR** enzymatic logic gates used in the present study can be scaled up to higher complexity by assembling enzymatic logic networks composed of several concatenated logic gates. The logic networks can accept many different chemical input signals and process chemical information according to the "program" embedded in the enzyme system. These systems represent a new generation of "smart" chemical devices that perform certain functions on demand, when the system operation is triggered by corresponding patterns of chemical signals. The reported system that performs oxidative damage upon activation by a combination of chemical signals will serve as a basis for development of smart systems capable of programmed detection, identification, and neutralization of potential biohazards.

Experimental Section

Chemicals and reagents: All enzymes were purchased from Sigma–Aldrich and were used as supplied. The enzymes that were used are: glucose oxidase (GOx) from *Aspergillus niger* type X-S (E.C. 1.1.3.4), esterase (Est) from porcine liver (E.C. 3.1.1.1), and crude catalase (Cat) from bovine liver (E.C. 1.11.1.6). Chemicals purchased from Sigma–Aldrich or Fluka were analytical quality and used as supplied: β-D-(+)-glucose, ethyl acetate, NTA, sodium ascorbate, benzoic acid, deoxyribose, thiobarbiturate. Chemicals purchased from J. T. Baker with ACS reagent grade were: ferrous sulfate ($FeSO_4$), sodium sulfate (Na_2SO_4). From Fisher was purchased certified ACS trichloroacetic acid. BHT ligand, 2,6-bis-[hydroxy-(methyl)amino]-4-(*N*-methyl, *N*-ethoxycarbonyl)amino-1,3,5-triazine, and its 2:1 iron complex, Fe^{III}–$(BHT)_2$, were prepared according to the known synthetic procedures.[46]

Apparatus: All measurements were performed at $37 \pm 0.1\,^{\circ}C$. The optical absorbance measurements were performed with a Shimadzu UV-2450PC spectrophotometer. The fluorescence spectra were recorded with a fluorescent spectrometer (Varian Inc.) using excitation at $\lambda = 305$ nm and measuring light emission spectra. The fluorescence intensity was normalized to the digital "**1**" value of the output signals. The pH evolutions were monitored with a Mettler Toledo® SevenEasy pH-meter.

Enzymatic logic gates composition and operation: Two different enzymatic logic gates were designed for the pH control. The biochemical "machinery" of the logic gates was defined as an aqueous solution (4 mL) containing Na_2SO_4 (10 mM); Fe^{III}–$(BHT)_2$ (0.15 mM); $FeSO_4$ (50 μM); NTA (50 μM); sodium ascorbate (5 mM) and the specific enzymes for each gate. The operation of the logic gates was performed at room temperature, $23 \pm 2\,^{\circ}C$. To perform the **AND** gate operation, GOx (40 units) was added to the machinery to get a final concentration of 10 units mL^{-1}. Catalase (1000 units) was also added. The two inputs triggering the **AND** gate operation were glucose—0 M and 20 mM for "**0**" input and "**1**" input, respectively, and oxygen—after bubbling Ar for 10 min as input "**0**" and in equilibrium with air as "**1**". To perform the **OR** gate operation, GOx (40 units) and Est (40 units) were added to the machinery to get a final concentration of 10 units mL^{-1} for each enzyme. Catalase (1000 units) was also added. The two inputs triggering the **OR** gate operation were glucose—0 M and 20 mM for "**0**" input and "**1**" input, respectively, and ethyl acetate—0 M and 20 mM for "**0**" input and "**1**" input, respectively. In the case of **OR** gate oxygen was always present in the system.

Acknowledgement

This research was supported by the NSF grant "Signal-Responsive Hybrid Biomaterials with Built-in Boolean Logic" (DMR-0706209).

Keywords: biocatalysis · enzymes · logic gates · oxidative damage · redox chemistry · switchable processes

[1] R. Baron, O. Lioubashevski, E. Katz, T. Niazov, I. Willner, *J. Phys. Chem. A* **2006**, *110*, 8548–8553.
[2] R. Baron, O. Lioubashevski, E. Katz, T. Niazov, I. Willner, *Angew. Chem.* **2006**, *118*, 1602–1606; *Angew. Chem. Int. Ed.* **2006**, *45*, 1572–1576.
[3] G. Strack, M. Pita, M. Ornatska, E. Katz, *ChemBioChem* **2008**, *9*, 1260–1266.
[4] X. G. Shao, H. Y. Jiang, W. S. Cai, *Prog. Chem.* **2002**, *14*, 37–46.
[5] A. Saghatelian, N. H. Volcker, K. M. Guckian, V. S. Y. Lin, M. R. Ghadiri, *J. Am. Chem. Soc.* **2003**, *125*, 346–347.
[6] G. Ashkenasy, M. R. Ghadiri, *J. Am. Chem. Soc.* **2004**, *126*, 11140–11141.
[7] A. P. De Silva, S. Uchiyama, *Nat. Nanotechnol.* **2007**, *2*, 399–410.
[8] A. Credi, *Angew. Chem.* **2007**, *119*, 5568–5572; *Angew. Chem. Int. Ed.* **2007**, *46*, 5472–5475.
[9] U. Pischel, *Angew. Chem.* **2007**, *119*, 4100–4115; *Angew. Chem. Int. Ed.* **2007**, *46*, 4026–4040.
[10] G. Strack, M. Ornatska, M. Pita, E. Katz, *J. Am. Chem. Soc.* **2008**, *130*, 4234–4235.
[11] T. Niazov, R. Baron, E. Katz, O. Lioubashevski, I. Willner, *Proc. Natl. Acad. Sci. USA* **2006**, *103*, 17160–17163.
[12] T. K. Tam, J. Zhou, M. Pita, M. Ornatska, S. Minko, E. Katz, *J. Am. Chem. Soc.* **2008**, *130*, 10888–10889.
[13] J. Zhou, T. K. Tam, M. Pita, M. Ornatska, S. Minko, E. Katz, *ACS Appl. Mater. Interfaces* **2009**, *1*, 144–149.
[14] M. Pita, M. Krämer, J. Zhou, A. Poghossian, M. J. Schöning, V. M. Fernández, E. Katz, *ACS Nano* **2008**, *2*, 2160–2166.
[15] M. Motornov, J. Zhou, M. Pita, V. Gopishetty, I. Tokarev, E. Katz, S. Minko, *Nano Lett.* **2008**, *8*, 2993–2997.
[16] M. Pita, S. Minko, E. Katz, *J. Mater. Sci.: Mater. Med.* **2009**, *20*, 457–462.
[17] K. Hensley, R. A. Floyd, *Arch. Biochem. Biophys.* **2002**, *397*, 377–383.
[18] M. K. Shigenaga, T. M. Hagen, B. N. Ames, *Proc. Natl. Acad. Sci. USA* **1994**, *91*, 10771–10778.
[19] D. A. Butterfield, J. Drake, C. Pocernich, A. Castegna, *Trends Mol. Med.* **2001**, *7*, 548–554.
[20] S. Przedborski, H. Ischiropoulos, *Antioxid. Redox Signaling* **2005**, *7*, 685–693.
[21] I. L. C. Chapple, *J. Clin. Periodontol.* **1997**, *24*, 287–296.
[22] K. A. Nath, S. M. Norby, *Am. J. Med.* **2000**, *109*, 665–678.
[23] A. C. Maritim, R. A. Sanders, J. B. Watkins, *J. Biochem. Mol. Toxicol.* **2003**, *17*, 24–38.
[24] M. Valko, M. Izakovic, M. Mazur, C. J. Rhodes, J. Telser, *Mol. Cellular Biochem.* **2004**, *266*, 37–56.
[25] M. S. Cooke, M. D. Evans, M. Dizdaroglu, J. Lunec, *FASEB J.* **2003**, *17*, 1195–1214.
[26] M. Dizdaroglu, P. Jaruga, M. Birincioglu, H. Rodriguez, *Free Radical Biol. Med.* **2002**, *32*, 1102–1115.
[27] L. J. Marnett, *Carcinogenesis* **2000**, *21*, 361–370.
[28] R. M. Adibhatla, J. F. Hatcher, *Free Radical Biol. Med.* **2006**, *40*, 376–387.
[29] M. Valko, D. Leibfritz, J. Moncol, M. T. D. Cronin, M. Mazur, J. Telser, *Int. J. Biochem. Cell Biol.* **2007**, *39*, 44–84.
[30] B. M. Babior, *Am. J. Med.* **2000**, *109*, 33–44.
[31] F. C. Fang, *Nat. Rev. Microbiol.* **2004**, *2*, 820–832.
[32] P. Wojtaszek, *Biochem. J.* **1997**, *322*, 681–692.
[33] G. Cairo, S. Recalcati, A. Pietrangelo, G. Minotti, *Free Radical Biol. Med.* **2002**, *32*, 1237–1243.
[34] F. C. Fang, *Nat. Rev. Microbiol.* **2004**, *2*, 820–832.
[35] J. P. Kehrer, *Toxicology* **2000**, *149*, 43–50.
[36] S. I. Liochev, I. Fridovich, *Redox Rep.* **2002**, *7*, 55–57.
[37] M. Hermes-Lima, E. M. Wang, H. M. Schulman, K. B. Storey, P. Ponka, *Mol. Cell. Biochem.* **1994**, *137*, 65–73.
[38] R. S. Britton, K. L. Leicester, B. R. Bacon, *Int. J. Hematol.* **2002**, *76*, 219–228.
[39] T. B. Chaston, D. R. Richardson, *Am. J. Hematol.* **2003**, *73*, 200–210.
[40] I. G. J. de Avellar, M. M. M. Magalhaes, A. B. Silva, L. L. Souza, A. C. Leitao, M. Hermes-Lima, *Biochim. Biophys. Acta Gen. Subj.* **2004**, *1675*, 46–53.
[41] D. R. Lloyd, D. H. Phillips, *Mutat. Res. Fund. Mol. Mechan. Mutagen.* **1999**, *424*, 23–36.
[42] T. B. Chaston, D. R. Richardson, *Am. J. Hematol.* **2003**, *73*, 200–210.
[43] I. Spasojevic, S. K. Armstrong, T. J. Brickman, A. L. Crumbliss, *Inorg. Chem.* **1999**, *38*, 449–454.
[44] I. Turcot, A. Stintzi, J. D. Xu, K. N. Raymond, *J. Biol. Inorg. Chem.* **2000**, *5*, 634–641.
[45] J. Gun, I. Ekeltchik, O. Lev, R. Shelkov, A. Melman, *Chem. Commun.* **2005**, 5319–5321.
[46] I. Ekeltchik, J. Gun, O. Lev, R. Shelkov, A. Melman, *Dalton Trans.* **2006**, 1285–1293.
[47] V. Privman, G. Strack, D. Solenov, M. Pita, E. Katz, *J. Phys. Chem. B* **2008**, *112*, 11777–11784.
[48] J. M. C. Gutteridge, *Biochem. J.* **1987**, *243*, 709–714.
[49] J. A. Simpson, K. H. Cheeseman, S. E. Smith, R. T. Dean, *Biochem. J.* **1988**, *254*, 519–523.

[50] B. Halliwell, M. Whiteman, *Br. J. Pharmacol.* **2004**, *142*, 231–255.
[51] W. Freinbichler, L. Bianchi, M. A. Colivicchi, C. Ballini, K. F. Tipton, W. Linert, L. Della Corte, *J. Inorg. Biochem.* **2008**, *102*, 1329–1333.
[52] A. Gomes, E. Fernandes, J. Lima, *J. Biochem. Biophys. Methods* **2005**, *65*, 45–80.
[53] J. E. Biaglow, Y. Manevich, F. Uckun, K. D. Held, *Free Radical Biol. Med.* **1997**, *22*, 1129–1138.
[54] M. Hermes-Lima, E. M. Wang, H. M. Schulman, K. B. Storey, P. Ponka, *Mol. Cell. Biochem.* **1994**, *137*, 65–73.
[55] M. J. Zhao, L. Jung, C. Tanielian, R. Mechin, *Free Radical Biol. Med. Res.* **1994**, *20*, 345–363.
[56] J. M. C. Gutteridge, *Biochem. J.* **1987**, *243*, 709–714.

Received: December 19, 2008
Published online on March 23, 2009

